Supporting Information

DARTE is available for download at dx.doi.org/10.7910/DVN/28999

1. Data Sources and Methodology

Vehicle Activity Data

The Highway Performance Monitoring System (HPMS) is a traffic monitoring program overseen by the Federal Highway Administration. All U.S. states and the District of Columbia are required to submit annual estimates for a wide variety of traffic and highway condition data to HPMS in compliance with federal statute. This data has been archived in a digital tabular format since 1980, and was made available to us upon request. The data format is described in detail in the HPMS Field Manual (1), which has been published and revised on a roughly 5 year cycle since 1977. The HPMS underwent significant revisions in 2010, with the most notable change being the requirement that states submit data in a GIS shapefile format. The HPMS dataset used to generate the 1980 – 2009 emissions estimates in DARTE is based on the old format of HPMS data, which is well described in the archived versions of the HPMS Field Manual (1). The raw HPMS data is unavailable for year 2010 due to issues associated with the transition to the GIS format. We imputed this data using the HPMS data from neighboring years as described below. For 2011 and 2012 we obtained the new GIS shapefile formatted HPMS data from FHWA and extracted the feature data into a tabular format compatible with the 1980 – 2009 data series. Data from all years was then merged into a single database.

The core data features of the HPMS are individual road segments that are defined by the state transportation departments. For each road segment HPMS reports the center-line length in miles, annual average daily traffic (AADT), functional class, urban/rural context, and county. AADT is a measure of the number of vehicles that traverse the road segment on an average day, adjusted for seasonal and day-of-week variation. Measurements of AADT are obtained from roads with permanent traffic recorders (PTRs) and from repeated short-term (48-72 hour) traffic counts performed throughout the year on other roads in the network. Data from PTRs is used to develop monthly, weekly, and day-of-week scaling factors that are then applied to short-term count data to obtain AADT values for neighboring roads that lack PTRs.

We calculated annual vehicle miles travelled (VMT) on each road segment in HPMS by multiplying AADT by the length of the road segment and then by 365 days. Since the individual road segments in HPMS were not explicitly geocoded until 2011, we aggregated road-segment VMT to the lowest common level of geography. There are 12 roadway functional classes included in HPMS (Table S1), six for urban roads and six for rural roads. Urban roads are defined as any road segment that falls partially or entirely within the boundaries of a Census Urbanized Area or Urban Cluster. We aggregated the HPMS data to counties by using the reported functional classes and a geocoded road network for the U.S. that is also partitioned by these functional classes.

Code	Description	Code	Description
RURAL		URBAN	
1	Principal Arterial - Interstate	11	Principal Arterial - Interstate
2	Principal Arterial - Other	12	Principal Arterial-Other Freeways & Expressways
6	Minor Arterial	14	Principal Arterial - Other
7	Major Collector	16	Minor Arterial
8	Minor Collector	17	Collector
9	Local	19	Local

Table S1. Highway Performance Monitoring System – Table of Roadway Functional Classification Definitions (1).

Although road segments in the 2011 and 2012 HPMS are individually geocoded, we chose to preserve the consistency and continuity of our emissions time series by performing the same aggregation by functional class and county and then merging all years of data into a uniformly formatted database. With the transition of HPMS to the GIS submission model, a subset of states submitted their 2009 HPMS data in the new GIS format. We performed a similar aggregation by functional class and county to this VMT, as was done with the 2011 and 2012 data. For 2010, there was no archived data from HPMS available; we linearly interpolate VMT between the 2009 and 2011 values of the HPMS raw data for each combination of county and urban/rural functional class.

The HPMS database does not include roadway-level data for many minor and local roads, as it was originally conceived as a highway-focused database. However, the archived data contains 'Summary Files' wherein states report VMT for rural and urban minor collectors, as well as urban local roads. State-level VMT for rural local roads is reported separately in Highway Statistics Table VM-2 (2). We integrate this state-level local road VMT data into our county-level database by allocating state totals by functional class to each county as shown in equations 1 and 2:

$$VMT_{c,f_{urban\ minor/local}} = VMT^{summary}_{s,f_{urban\ minor/local}} \times \frac{\sum_{f_{urban}} VMT^{hpms}_{c,f}}{\sum_{f_{urban}} VMT^{hpms}_{s,f}} \quad \text{(eqn. 1)}$$

$$VMT_{c,f_{rural\ minor/local}} = VMT^{summary}_{s,f_{rural\ minor/local}} \times \frac{\sum_{f_{rural}} VMT^{hpms}_{c,f}}{\sum_{f_{rural}} VMT^{hpms}_{s,f}} \quad \text{(eqn. 2)}$$

Where:

- $VMT^{summary}_{s,f_{urban\ minor/local}}$ is the total VMT for urban minor collectors or local roads in state ***S*** reported in the HPMS Summary Files
- $\sum_{f_{urban}} VMT^{hpms}_{c,f}$ is the sum of all urban road VMT reported to HPMS for county ***C***
- $\sum_{f_{urban}} VMT^{hpms}_{s,f}$ is the sum of all urban road VMT reported to HPMS for state ***S*** that contains county ***C***
- $VMT^{summary}_{s,f_{rural\ minor/local}}$ is the total VMT for rural minor collectors or local roads in state ***S*** reported in the HPMS Summary Files or Highway Statistics Series Table VM-2, respectively
- $\sum_{f_{rural}} VMT^{hpms}_{c,f}$ is the sum of all rural road VMT reported to HPMS for county ***C***
- $\sum_{f_{rural}} VMT^{hpms}_{s,f}$ is the sum of all rural road VMT reported to HPMS for state ***S*** that contains county ***C***

The resulting database contains a complete VMT time series for every functional class of road present in each county for the years 1980 – 2012.

2. Data Quality Assurance & Control

We inspected the complete time series of VMT by county and functional class to identify potential outliers or structural breaks in the dataset. We developed a filtering algorithm that flagged any observation in an individual county/functional class time series if the magnitude of the year-on-year difference between an observation and adjacent years was greater than two standard deviations from the mean year-on-year difference of that time series. For these single points that deviated significantly from the trend of the series, we removed the value and replaced it with an imputed value obtained by fitting a lowess curve to the full time series minus the removed value.

In some cases, we observed apparent structural breaks in a county/functional class time series when a county or state reclassified roads to a different functional class, thereby shifting a significant amount of VMT to that

new class. This occurred most often in the years following a Decennial Census, when the boundaries of Urbanized Areas were revised and roads that were previously classified as rural were shifted to the urban equivalent of their previous functional class. In those cases, there was no observed break in the state's time series for total VMT, and our algorithm did not generate a flag. However, visual inspection of the data noted the presence of a small number of genuine structural breaks that could not be explained by road reclassification. These cases tended to be similar in style to the single outlier observations described above, but instead of a single errant observation we observed small clusters of 2-4 observations that were bookended by large, oppositely signed deviations from the main trend of the time series. The filtering algorithm identified these in the same manner as the single outliers, with the similar condition that no concurrent and complementary deviations were present on any other road classes in that county. These observations were similarly dropped and imputed using values from a lowess fit to the series minus the outlying cluster. Of the 761,759 observations in the dataset, roughly 10% were flagged and replaced by our filtering procedure.

3. Partitioning VMT by vehicle type

For each year, county, and functional class, we partitioned annual VMT from HPMS into the five vehicle types used by the Highway Statistics Series Table VM-4 (3): Passenger cars, passenger trucks (SUV, pickups, mini-vans), buses, single-unit trucks, and combination trucks. Motorcycle VMT was included with passenger cars. The values in Table VM-4 were estimated by state transportation departments based on vehicle classification studies, transit agency data, the number of registered vehicles of each type in the state, and data on interstate freight travel. These vehicle type estimates can be used to calculate the total volume of fuel consumed by each vehicle class by dividing VMT by vehicle fuel economy. However, using the reported vehicle shares and the average fuel economies for each vehicle type (4) produced gasoline and diesel consumption totals that did not match the values reported in Highway Statistics Table MF-21 (5) for most states. As Table MF-21 is based on state tax revenue from fuel sales, we considered it to be the most reliable estimate of fuel consumption at the state level. To correct for this mismatch, we developed a calibration routine to make small adjustments to the reported vehicle shares and fuel economies for each state, such that the resulting calculations of gasoline and diesel consumption for each state were within ± 5% of the values reported in Table MF-21. This routine was developed and performed using the CONOPT optimization routine in the software package GAMS.

4. Vehicle shares calibration routine

The calibration routine is initialized using the reported values for vehicle shares taken from the Highway Statistics Series Table VM-4. For years prior to 1993, initial values for vehicle shares of VMT are assigned the values reported in the 1993 Table VM-4, the first year that this table was published. Attempts were made to initialize the model using national average vehicle shares reported in Highway Statistics Series Table VM-1 (4), which are available for 1980-1993, but model convergence and calculations of fuel consumption was found to be extremely poor. Our review of state-level vehicle shares in Table VM-4 showed that there is significant variation about the national mean for vehicle shares, and therefore the national average is not a sufficiently precise representation of local vehicle fleet VMT distributions. We used the 1993 Table VM-4 values for each state for the years prior to 1993. For the years 1993-1997, we used vehicle shares reported in each year's Table VM-4. For the years 1998-2008, publication of Table VM-4 was temporarily suspended. Publication was then resumed in the year 2009. For each state and functional class, we linearly interpolated vehicles shares between the 1997 and the 2009 and used those values to initialize the model for the intervening years. For years after 2009 we use the published VM-4 shares.

National average fuel economies for each vehicle type were obtained from (4). For passenger cars and passenger trucks we assumed all fuel consumption is motor gasoline. For buses and combination trucks we assumed all fuel consumption is diesel fuel. Single-unit truck VMT was split into diesel and gasoline shares using data from the Vehicle Inventory and Use Survey (VIUS) conducted in the years 1982, 1987, 1992, 1997 and 2002 (6). For the years prior to 1982, the 1982 share was used. For years between 1982 and 2002, we interpolated

the shares linearly between each VIUS. Since VIUS was discontinued in 2002, for years after 2002 we used the value from the 2002 VIUS.

Optimization of vehicle shares and fuel economies was performed annually, starting with 1980. The initial values for each year were provided as described above. The calibration routine used this initial data to calculate gasoline and diesel consumption for each vehicle type in each functional class for each state. Gas and diesel consumption was then summed to the state level for each year. For each year the model minimized the sums of squared deviations between initial and optimized values for vehicle fuel economies, gasoline and diesel consumption, and single-unit truck gas/diesel share, subject to the following constraints:

1. Final calculated state totals of gas and diesel consumption must be within 5% of state totals published in Highway Statistics Series Table MF-21.
2. Fuel economy for each vehicle type must be within 3 miles per gallon of national average for that vehicle type.
3. Year-on-year changes to the share of VMT for any given vehicle type could not be more or less than 10% of previous year's share for that vehicle type.
4. Total VMT by functional class in each state must match exactly the reported values from Highway Statistics Series Table VM-2 (2).

Fuel economies, vehicle shares, and single-unit truck gas/diesel split for each functional class of road in each state were adjusted from initial values by the routine, subject to the above constraints. State totals of VMT by functional class were not altered. This routine's output included calibrated values for the vehicle shares of VMT for each functional class and state, the fuel economies for each vehicle type by functional class and state, and the single-unit truck gas/diesel split by state. We then applied these values to our full HPMS dataset of VMT at the county/functional class level.

The HPMS dataset partitions VMT across 12 functional classes of road, but vehicle shares in Table VM-4 were reported only for a more aggregated set of 5 functional classes. The output of the calibration routine was similarly partitioned by these 5 functional classes, and we used a crosswalk table (Table S2) to assign the calibrated vehicle shares and fuel economies to all county/functional class pairs in the HPMS database. All counties within a state were assigned the same state-level vehicle shares and fuel economies by functional class for a given year.

Highway Statistics Series			**Highway Performance Monitoring System**	
Code	*Description*		*Code*	*Description*
1	Rural Interstates and Freeways		1	Rural Principal Arterial - Interstate
2	Rural Principal Arterials		2	Rural Principal Arterial - Other
3	Rural Other Arterials		6	Rural Minor Arterial
3	Rural Other Arterials		7	Rural Major Collector
3	Rural Other Arterials		8	Rural Minor Collector
3	Rural Other Arterials		9	Rural Local Road
4	Urban Interstates and Freeways		11	Urban Principal Arterial - Interstate
4	Urban Interstates and Freeways		12	Urban Arterial - Other Freeways & Expressways
5	Urban Other Arterials		14	Urban Principal Arterial - Other
5	Urban Other Arterials		16	Urban Minor Arterial
5	Urban Other Arterials		17	Urban Collector
5	Urban Other Arterials		19	Urban Local Road

Table S2. Crosswalk table between functional classifications used for roads in Highway Statistics Series Tables VM-1 and VM-4 and the functional classifications system used in the Highway Performance Monitoring System.

VMT for each county / functional class was partitioned across the five vehicle types, and motor gasoline and diesel fuel consumption was calculated using the fuel economies for each vehicle type. Single-unit truck VMT was further partitioned into gasoline and diesel shares, with fuel consumption calculated separately. The same fuel economy was used for both gasoline and diesel single-unit trucks in a given state and functional class of road. Total gasoline and diesel consumption for each county and functional class was converted to emissions of CO_2 using emissions factors of 8.91 kg CO_2 gallon^{-1} gasoline and 10.15 kg CO_2 gallon^{-1} diesel (7). Emissions from gasoline and diesel consumption were summed by county and functional class for assignment to the GIS road network.

We used 2012 Census TIGER/Line road shapefiles for all states in the coterminous U.S. The TIGER road network classifies roads using only 3 functional classes, and does not distinguish between urban and rural roads. We therefore intersected the TIGER road shapefile with a polygon shapefile of the Census 2000 Urbanized Areas and Urban Clusters to add an urban/rural classification to each TIGER road segment. Next we aggregated our HPMS-based emissions to the 3 urban and 3 rural functional classes of the TIGER road network as shown in Table S3.

MFCC Code	*Description*		*Code*	*Description*
S1100	Primary Road		1	Rural Principal Arterial - Interstate
S1100	Primary Road		2	Rural Principal Arterial - Other
S1200	Secondary Road		6	Rural Minor Arterial
S1200	Secondary Road		7	Rural Major Collector
S1400	Local Road		8	Rural Minor Collector
S1400	Local Road		9	Rural Local Road
S1100	Primary Road		11	Urban Principal Arterial - Interstate
S1100	Primary Road		12	Urban Arterial - Other Freeways & Expressways
S1100	Primary Road		14	Urban Principal Arterial - Other
S1200	Secondary Road		16	Urban Minor Arterial
S1200	Secondary Road		17	Urban Collector
S1400	Local Road		19	Urban Local Road

Table S3. Crosswalk table between functional classification systems of Census TIGER/Line road network and HPMS.

We calculated the total length in kilometers of each functional class of road in each county in the TIGER network, and divided our CO_2 emissions by this length to obtain per-kilometer emissions for each year/county/functional class. These per-km emissions were then assigned to all segments in the TIGER road network. The road network was intersected with a 1 x 1 km grid and a 0.01 x 0.01 degree grid, and the new lengths of the road segments within each grid cell were calculated. Total emissions for each grid cell were obtained by multiplying the new road segment lengths by the per-kilometer emissions assigned to each segment and then summing by grid cell.

Both the 1km and 0.01 degree DARTE grids were based on the grids used by the Vulcan (8) and EDGAR (9) emission inventories, respectively. The 1km grid has the same datum and geographic projection as the Vulcan grid, and is an even division of the Vulcan 10km grid cells, such that all cell boundaries overlap exactly. The same is the case with the 0.01 degree grid with respect to the EDGAR 0.1 degree grid. This was done so that DARTE can be easily compared and combined with Vulcan and EDGAR emissions from other sectors without the need for re-gridding.

5. Comparison of DARTE with EDGAR and Vulcan inventories

National on-road CO_2 emissions totals for DARTE, the EDGAR and Vulcan inventories, the EPA national greenhouse gas inventory (10), and emissions calculated from FHWA state-level fuel consumption data (5) show broadly consistent patterns in time (Figure S1). DARTE emissions are within 3% of EPA and FHWA values, while EDGAR emissions are systematically lower than DARTE, EPA, and FHWA, with an average annual deviation of 8%.

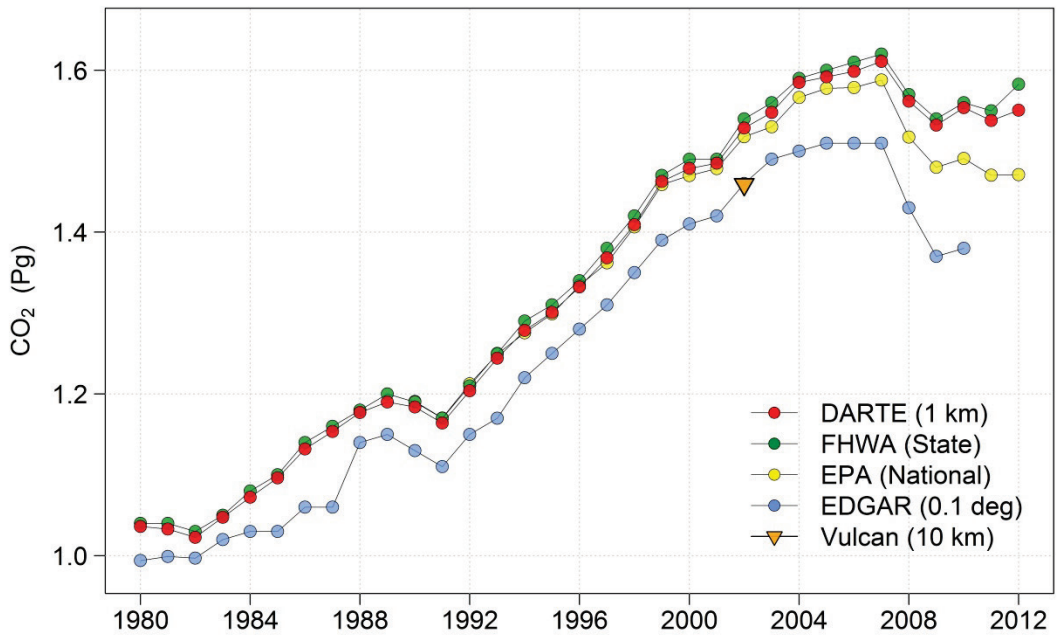

Figure S1. Comparison of total national on-road CO_2 emissions reported by DARTE with the EDGAR and Vulcan Inventories, the EPA national greenhouse gas inventory and emissions calculated from FHWA state-level fuel consumption data (5). The spatial resolution of each inventory is shown parenthetically in the legend.

To examine the sub-national differences between EDGAR and DARTE emissions, DARTE was aggregated to the 0.1 degree EDGAR grid, and grid cells were classified based on the fraction of each cell's overlap with the U.S. Census 2000 Urbanized Areas and Urban Clusters. Although national emission totals were similar for DARTE and EDGAR (Figure S1), when they were compared on a cell-by-cell basis large deviations in emissions were observed, with EDGAR exceeding DARTE by as much as 500% in some locations (Figure S2). There was a systematic positive bias of EDGAR emissions in urban areas relative to DARTE, with over 30% of cells in the 75% urban category having EDGAR emissions that exceeded DARTE by more than 50%. For a full 25% of all grid cells EDGAR emissions exceeded DARTE by greater than 50%. The relative biases in EDGAR emissions for rural cells were similarly large, but less systematic: 40% of rural cells had EDGAR emissions 50% lower than DARTE and 29% of rural cells had EDGAR emissions 50% higher than DARTE.

EDGAR's use of road density as a sole proxy assumes a uniform emission factor per kilometer of road, which causes CO_2 to be over-allocated to low-traffic roads and under-allocated to high-traffic roads. This is most clearly visible across the Midwest and the rural Southeast (Figure S3), where EDGAR emissions showed a large negative bias relative to DARTE in grid cells containing major interstate highways (green), and a positive bias in grid cells dominated by local rural roads (orange). These deviations demonstrate the mismatch between road extent and vehicle activity that occurs at this scale. Symmetrically, in large urban areas EDGAR's estimates significantly exceeded DARTE in city centers while underestimating at the suburban and exurban fringes. Although many urban roads carry large amounts of traffic, and hence are responsible for the majority of emissions, urban areas also contain a large number of local roads which are comparatively lightly travelled. EDGAR's use of a constant emission factor across road classes with very different activity levels is likely the main source of the large spatial

biases we observed relative to DARTE. Overall, the spatial structure of EDGAR on-road emissions does not appear to be consistent with the spatial patterns of the underlying emission-generating source activity.

Aggregating DARTE's 2002 CO_2 estimates to Vulcan's 10km grid revealed similarly large spatial differences in emissions, with Vulcan estimates exceeding DARTE by 50% or greater in nearly 40% of grid cells. However, in contrast to EDGAR, we found that Vulcan emissions showed large negative biases relative to DARTE in the cores of large cities, and large positive biases in the surrounding suburban and exurban areas (Figure S2). Vulcan emissions in rural areas of the western United States show good agreement with DARTE on average, however, as with EDGAR, Vulcan displayed a large negative bias relative to DARTE on most of the rural interstate highway network (Figure S4). The differences between Vulcan and DARTE are most likely explained by how the VMT used by Vulcan to estimate on-road emissions was spatially downscaled from state and Urbanized Areas to counties in the NCD (see discussion in main text).

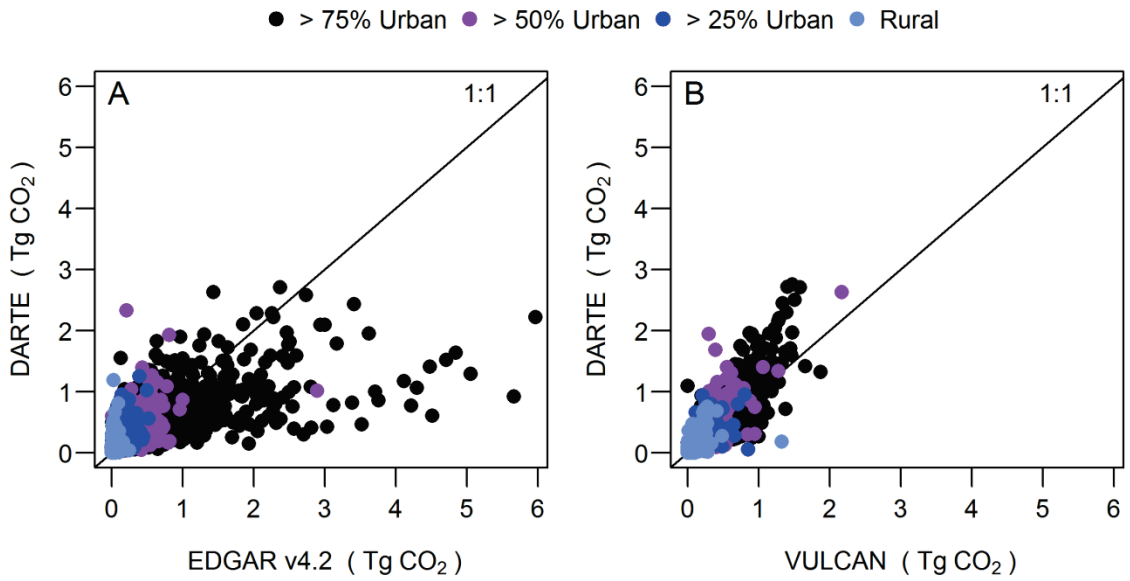

Figure S2. Cell-by-cell comparison of DARTE with EDGAR v4.2 (0.1° grid) and Vulcan (10 km grid). Grid cells were classified by their percent area of overlap with U.S. Census Urbanized Areas or Urban Clusters. DARTE – EDGAR comparison is for year 2008 emissions. DARTE – Vulcan comparison is for year 2002 emissions.

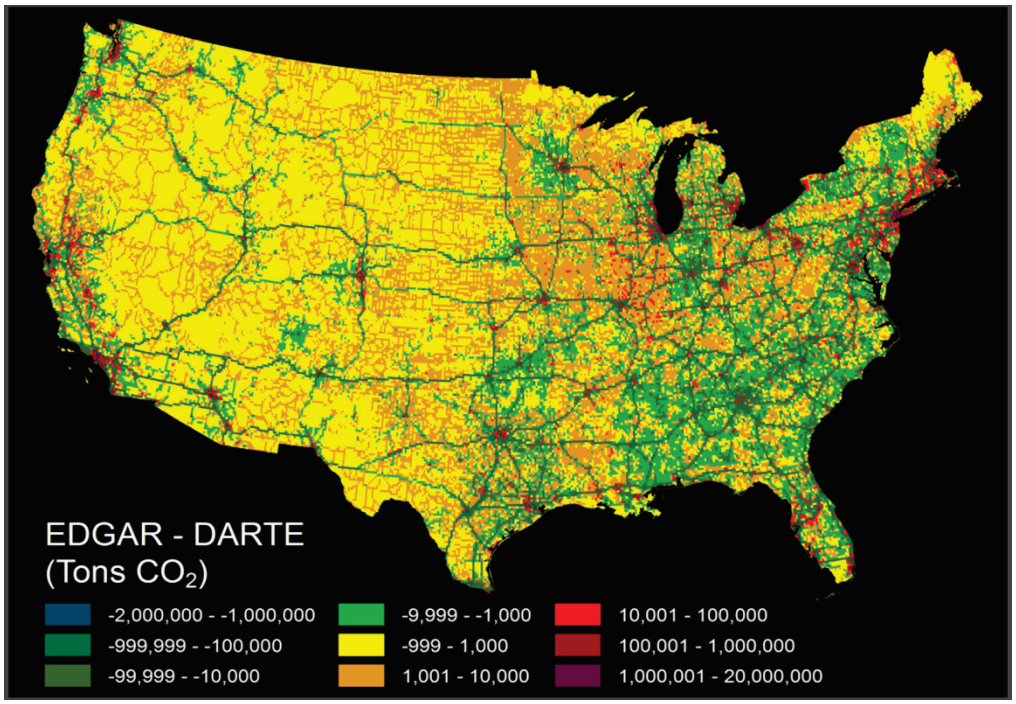

Figure S3. Cell-by-cell difference between EDGAR and DARTE for the year 2008; 2008 is the most recent year for which EDGAR v4.2 estimates are available. Resolution is 0.1° x 0.1° on the native EDGAR grid. Green areas indicate cells where EDGAR showed a negative bias relative to DARTE; orange and red areas show cells with a positive bias relative to DARTE. Differences are largest in the major urban areas.

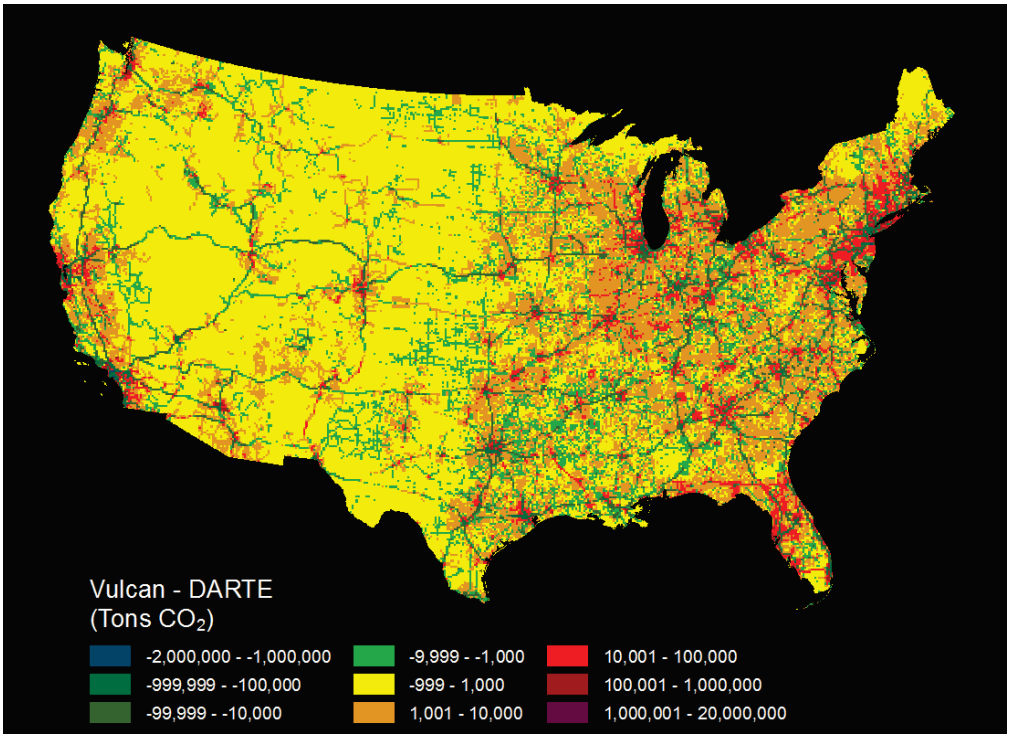

Figure S4. Cell-by-cell difference between Vulcan and DARTE for the year 2002. Green areas indicate cells where Vulcan under-allocated emissions relative to DARTE, orange and red cells show where Vulcan over-allocated emissions relative to DARTE.

6. Generalized Additive Model

We estimated two generalized additive models using on-road CO_2 emissions from DARTE. In the first model, **GAM_1,** we regressed total county-level on-road CO_2 emissions on lagged values of population density, per-capita income (in constant 2009 dollars), retail job density, non-retail job density and annual change in population (the last term being defined as the county population in the previous year minus the population in the year before that). The second model, **GAM_2**, we regressed per-capita on-road CO_2 emissions on the same variables. Non-retail jobs were calculated as the sum of all jobs in a county not classified as retail. All employment and income data were obtained from the Bureau of Economic Affairs Regional Data Tables (http://www.bea.gov/iTable/index_regional.cfm).

GAM_1:

$$\mathrm{CO_2}_{\,i,t} = \alpha_i + \tau_t + \Psi_1\left[\begin{pmatrix}\text{Population}\\ \text{density}\end{pmatrix}_{i,t-1}\right] + \Psi_2\left[\begin{pmatrix}\text{Per-capita}\\ \text{income}\end{pmatrix}_{i,t-1}\right] + \Psi_3\left[\begin{pmatrix}\text{Retail jobs}\\ \text{per km}^2\end{pmatrix}_{i,t-1}\right] + \Psi_4\left[\begin{pmatrix}\text{Non-retail jobs}\\ \text{per km}^2\end{pmatrix}_{i,t-1}\right] + \Psi_5\left[(\text{Population})_{i,t-1} - (\text{Population})_{i,t-2}\right] + \varepsilon_{i,t}$$

GAM_2:

$$\text{Per-capita } \mathrm{CO_2}_{\,i,t} = \alpha_i + \tau_t + \Psi_1\left[\begin{pmatrix}\text{Population}\\ \text{density}\end{pmatrix}_{i,t-1}\right] + \Psi_2\left[\begin{pmatrix}\text{Per-capita}\\ \text{income}\end{pmatrix}_{i,t-1}\right] + \Psi_3\left[\begin{pmatrix}\text{Retail jobs}\\ \text{per km}^2\end{pmatrix}_{i,t-1}\right] + \Psi_4\left[\begin{pmatrix}\text{Non-retail jobs}\\ \text{per km}^2\end{pmatrix}_{i,t-1}\right] + \Psi_5\left[(\text{Population})_{i,t-1} - (\text{Population})_{i,t-2}\right] + \varepsilon_{i,t}$$

The fitted splines for the lagged population density component from each model across the full range of U.S. county population densities are shown in Figure S5. The fitted splines for the other independent variables in both models (Figure S6) and the summary statistics (Table S4) for each model are reported. The estimated splines are non-parametric estimates of the partial component of emissions explained by each independent variable, relative to the conditional mean. The shape of each spline describes the average within-county effect of the independent variable on total or per-capita emissions across all counties and years in the dataset. For total CO_2 emissions we find that retail employment density is negatively correlated with emissions, and that non-retail employment density is positively correlated with emissions in all counties except New York City.. Non-retail employment and population density are the two largest contributors to total emissions as estimated by our model. Per-capita income has a small positive contribution to total emissions for incomes between $30,000 and $60,000, and a negative contribution at incomes greater than $60,000. The lagged annual population growth term shows a minimal influence on total emissions for most counties, but for fast-growing counties the effect is positive with lagged annual growth of 50,000 – 125,000, then becomes negative at higher levels. For per-capita emissions, per-capita income initially has a negative effect at low incomes and then becomes a positive effect for incomes above $30,000. Retail employment density is positively associated with per-capita emissions, but the effect plateaus at ~400 retail jobs per km^2. Non-retail employment density has a negative association with per-capita emissions, although the effect is largely stable across most counties at ~ -5 Tg-person^{-1}-km^{-2}. Lagged population growth had no statistically significant effect on per-capita emissions.

The rug plots along the x-axis in each panel in Figure S5 reveal the heavily skewed distribution of population density for U.S. counties. Despite increasing growth of large urban areas, in 2012, over 87% of the U.S. population still lived in counties with densities of less than 1,000 persons-km^{-2}, a share that has not changed significantly since 1980 (Figure S7). Our results show that increasing density is associated with an increase in

total county emissions of on-road CO_2 until densities exceed 1,650 persons-km^{-2}, while the decreasing trend in per-capita emissions with density appears to level out and stabilize once densities exceed 1,200 persons-km^{-2}. Only at the high densities of the largest cities in the U.S. (2,000 – 4,000 persons-km^{-2}) do we observe decreases in per-capita emissions large enough to offset increasing total CO_2 emissions. For low-density towns and counties that are attempting to reduce future on-road emissions by increasing population densities in their urban areas, our results offer the caution that the per-capita decreases associated with densification may not provide the reductions in total vehicle travel that earlier research on this topic seemed to promise (11).

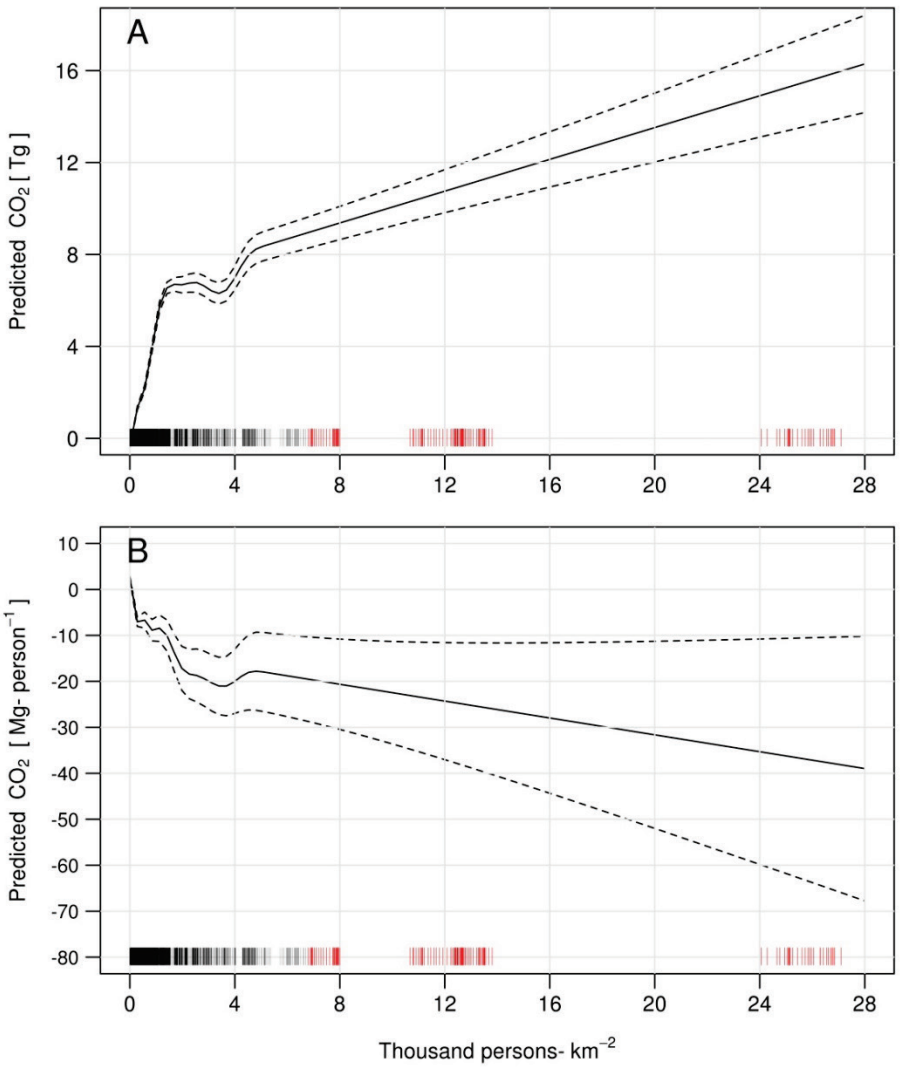

Figure S5. Comparison of fitted splines for total emissions versus population density (Panel A) and per-capita emissions versus population density (Panel B), as estimated by the generalized additive models described in the main text. The increase in total emissions with density begins to plateau at 1,650 persons-km^{-2}, before rising sharply again at 4,000 persons-km^{-2}. Per-capita emissions decrease rapidly for densities less than 250 persons-km^{-2}, but then decrease much more slowly between 250 and 1,200 persons-km^{-2}. The rapid decrease resumes at 1,200 persons-km^{-2} and continues before flattening slightly at 2,000 persons-km^{-2} and then plateauing until 8,000 persons-km^{-2}. The rug plot at the base of both graphs shows the pooled distribution of population density across all U.S. counties and years covered by DARTE. The red ticks in the rug plots denote counties that comprise parts of New York City, NY.

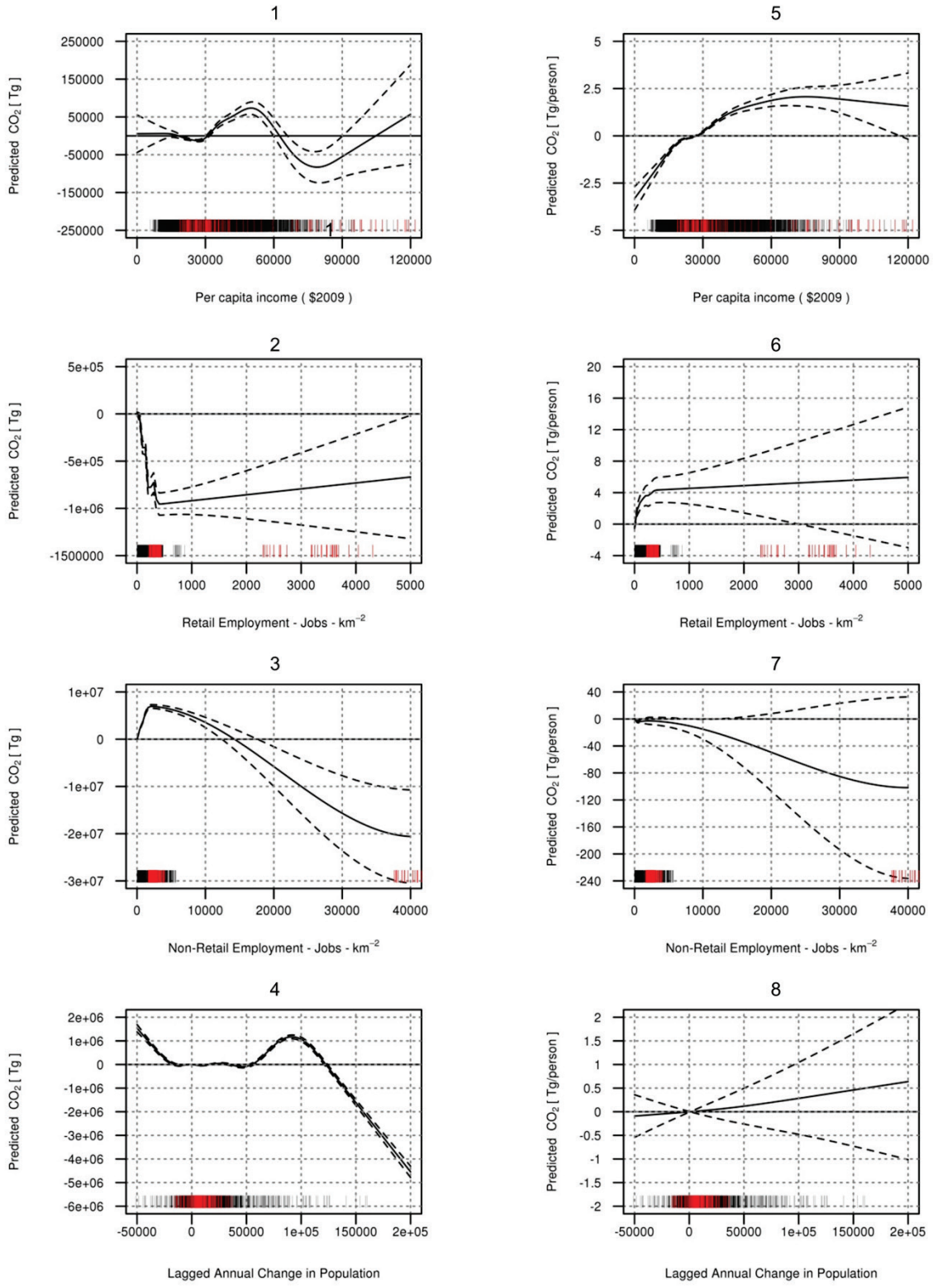

Figure S6. Plot of smooth terms $(\Psi_2\text{-}\Psi_5)$ in GAM_1 (total emissions - left column, Panels 1-4), and GAM_2 (per-capita emissions - right column, Panels 5-8). Rug plots show distribution of county values for each independent variable, pooled over all years. Red tick marks in the rug plots represent the counties that comprise New York City, NY.

GAM_1	*Effective Degrees of Freedom*	*Reference Degrees of Freedom*	*p-value*	GAM_2	*Effective Degrees of Freedom*	*Reference Degrees of Freedom*	*p-value*
Ψ_1	8.987	9.000	< 2E-16	Ψ_1	9.000	9.000	< 2E-16
Ψ_2	8.562	8.947	< 2E-16	Ψ_2	7.792	8.640	< 2E-16
Ψ_3	8.881	8.994	< 2E-16	Ψ_3	8.892	8.994	3.36E-13
Ψ_4	8.981	9.000	< 2E-16	Ψ_4	8.048	8.710	4.73E-07
Ψ_5	8.929	8.999	< 2E-16	Ψ_5	1.160	1.306	0.707
Adj-R^2 = 0.98	Generalized Cross Validation (GCV) = 3.29E10			Adj-R^2 = 0.88	Generalized Cross Validation (GCV) = 6.16		

Table S4. Summary statistics for the smooth terms in each GAM specification.

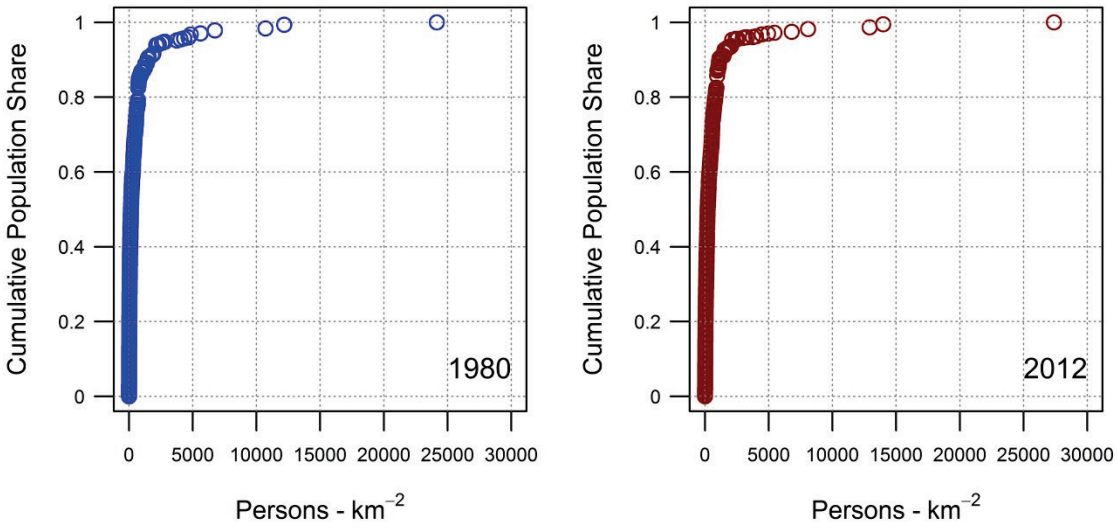

Figure S7. Cumulative population as share of U.S. total vs. population density for U.S. counties in 1980 (left) compared to in 2012 (right). Over 85% of the U.S. population resided in counties with densities less than 1,000 persons-km^{-2} in 2012. Population growth in low-density counties in the South and Central U.S. has resulted in the urbanization of small- and medium-sized cities with population densities that are typically associated with high per-capita transportation energy consumption and related carbon emissions. As a consequence, despite the overall growth in urban populations since 1980, the total distribution U.S. population by density has not substantially shifted towards the denser urban core counties.

7. Public Transit and Emissions

To investigate the potential influence of transit ridership on per-capita on-road CO_2 emissions we made use of decadal Census long-form survey responses on the percentage of workers who commute by private vehicle, carpool, public transit, or other modes (cycling, walking, motorcycle). For the years 1990, 2000 and 2010, this data is available at the Census Designated Place level of geography (12-13) (Figure S8 and Fig 4C in the main text). Trends in per-capita emissions as a function of transit commuters per person (Figure 4C) and the share of workers over the age of 16 who commute by public transit (Figure S8) show similar trends, although we observe differences in the magnitude of change in transit shares when we only consider the mode choice of commuter trips. Per-capita emissions appear to decrease somewhat slower with increasing transit use by commuters, however as commuting only comprises ~28% of national VMT on average (14), this is not surprising. Cities with

high population density are also the cities with the highest per-capita transit mode share, and these cities tend to have lower per-capita on-road CO_2 emissions. For the cities with lower population density and lower transit mode share, we observed higher per-capita emissions in the more recent data (2000 and 2010). The results in Figure 4C and Figure S8 provide evidence for a modest correlation between population density, public transit usage and per-capita emissions, and for cities that are already relatively dense the correlation appears be negative over time. However, due to the limited sample size available, it is difficult to rigorously quantify the transit-emissions relationship, particularly in the low density cities and counties that have experienced the greatest amount of population growth across the past decade.

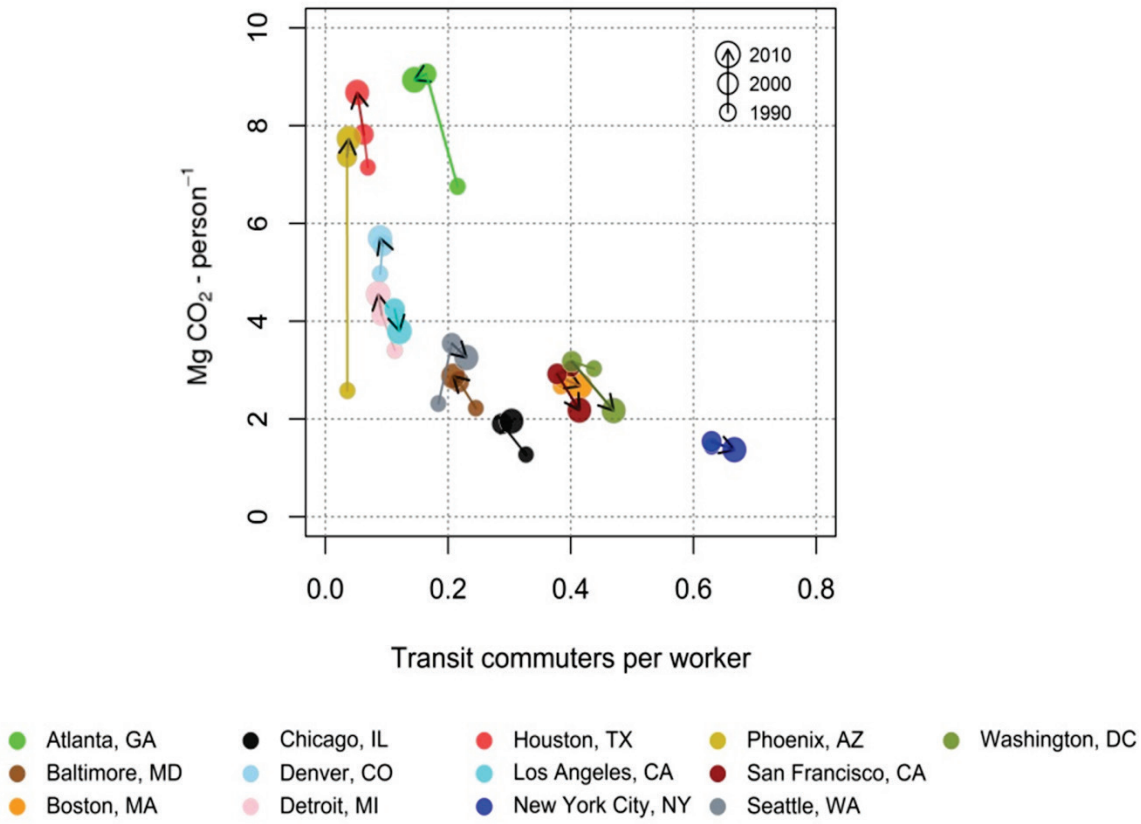

Figure S8. Plot of on-road CO_2 emissions per person vs. the share or workers over the age of 16 who commute by public transit, in 1990, 2000 and 2010 for a sample of U.S. cities.

Note, we were not able to include data on ridership levels from different transit systems as part of our regression modeling analysis due to limitations in data collection by public transit agencies across the United States.The National Transit Database maintained by the Federal Transit Administration is the best data source for systematic transit ridership, however the data is aggregated by agency and by Census Urbanized Area Disaggregating data from the Urbanized Area scale to the county scale would have introduced significant bias, as many transit systems in large cities span multiple counties, and there is no information available on the distribution of ridership across the system.

8. Ranking of counties by emissions

Over 50% of U.S. on-road CO_2 emissions occur in just 7% of counties. In 2012 the top 10 highest emitting counties were responsible for 10% of all national emissions (Table S5). Compared to the rest of the U.S., the top ten counties have lower per-capita emissions for both gasoline and diesel vehicle CO_2, but have both higher road densities and higher emissions per kilometer of road than the rest of the country, offsetting the below-average per-capita emissions and contributing to their large total emission levels. With the exception of San Bernardino County, CA, all of these counties have population densities higher than the national average, and in most cases they contain large urban areas where population densities are even significantly higher. Despite the high densities and below-average per-capita emissions rates, the sheer number of people residing and driving in these counties means that their total level of on-road emissions is high.

County	Tons CO_2	Pop. Density (per km^2)	Road Density (km per km^2)	CO_2 per capita (tons)			CO_2 per road-km (tons)			CO_2 per VMT (grams)		
				Total	*Gasoline*	*Diesel*	*Total*	*Gasoline*	*Diesel*	*Total*	*Gasoline*	*Diesel*
1. Los Angeles, CA	39,447,761	947.9	4.7	4.0	3.4	0.6	799.6	679.5	120.0	497.6	422.9	74.7
2. Harris, TX	19,354,340	964.1	7.4	4.6	3.6	0.9	590.1	469.3	120.9	560.0	445.3	114.7
3. Cook, IL	17,679,211	2,136.7	10.9	3.4	2.6	0.7	663.6	519.3	144.2	491.4	384.6	106.8
4. Maricopa, AZ	16,179,572	165.4	1.9	4.1	3.4	0.7	358.7	295.8	62.9	480.7	396.4	84.3
5. San Diego, CA	13,965,639	291.6	2.4	4.4	3.6	0.8	530.9	438.3	92.6	504.9	416.8	88.1
6. Orange, CA	13,178,336	1509.2	7.6	4.3	3.7	0.6	842.9	723.8	119.1	495.3	425.3	70.0
7. Dallas, TX	12,878,332	1087.4	7.8	5.2	4.2	1.1	727.6	580.3	147.3	559.3	446.0	113.3
8. San Bernardino, CA	11,013,708	40.1	0.9	5.3	4.1	1.2	229.7	179.5	50.1	522.0	408.0	113.9
9. Riverside, CA	10,548,353	121.6	1.4	4.6	3.7	1.0	393.5	312.7	80.9	517.0	410.8	106.2
10. Miami-Dade, FL	9,071,230	527.2	3.0	3.5	3.0	0.5	617.3	535.5	81.9	452.4	392.4	60.0
Rest of U.S.	*1,386,722,431*	*99.7*	*1.8*	*8.2*	*5.5*	*2.7*	*125.4*	*92.8*	*32.6*	*550.2*	*389.8*	*160.4*

Table S5. Top ten highest-emitting counties in 2012. These counties also comprise 10% of the U.S. population, but have lower per-capita emissions and higher road and population densities than the average of the remaining 3,094 counties. Total and average emissions reflect contributions from both diesel and gasoline vehicles.

9. Uncertainty of VMT

Vehicle miles travelled estimates in HPMS are derived from a combination of PTRs and short-term traffic counts conducted with portable sensors. PTRs provide year-round data on traffic activity and are considered to measure total volumes with 95%-99% accuracy (15). These data are used to derive seasonal and day-of-week factors to convert short-term counts into annualized average daily traffic (AADT) values. For roads whose traffic is not directly measured, AADT is imputed from similar roads nearby that have been directly measured (1). FHWA requires all AADT estimates submitted to HPMS to meet precision and accuracy standards that vary by roadway functional class: Freeways and larger roads are required to be accurate within 5%, while local rural road AADT must be within 15% (1).

Total emissions for each road class in each county were assigned to the TIGER/Line road network by dividing the total emissions on functional class *f*, in county *c*, by the total length of roads of functional class *f* in county *c*,

and then applying the resulting per-kilometer emissions factor to all roads of class *f* in county *c*. This procedure averaged out the local variation in per-kilometer emissions across roadway segments within each functional class. To estimate the potential uncertainty associated with this process we calculated the coefficient of variation (CV) for VMT on each functional class within each county for each year using roadway-level VMT from the HPMS archive. We then averaged the annual CVs across all years in the dataset and plotted them on a national map (Figure S9). We found that for most U.S. counties, the within-county variation in VMT was low for rural freeways and for urban roads in general. The largest variation was seen on rural non-freeway road classes, with Indiana, Alabama, Vermont and Idaho showing the largest within-county variation on these roads. Rural non-freeway road segments are typically the least-sampled roads in HPMS, and are held to lower standards of precision according to the guidelines in the HPMS Field Manual (1). This would account for the overall larger values of CV on these roads, but there are also clear state-specific deviations that suggest data from certain states may be less precisely collected than in others. Rural non-freeways only accounted for 17% of total VMT (and 17% of total CO_2 emissions) in 2012, so while the spatial uncertainty of emissions from these roads is larger than other functional class roads, the overall contribution to total emissions uncertainty is relatively small.

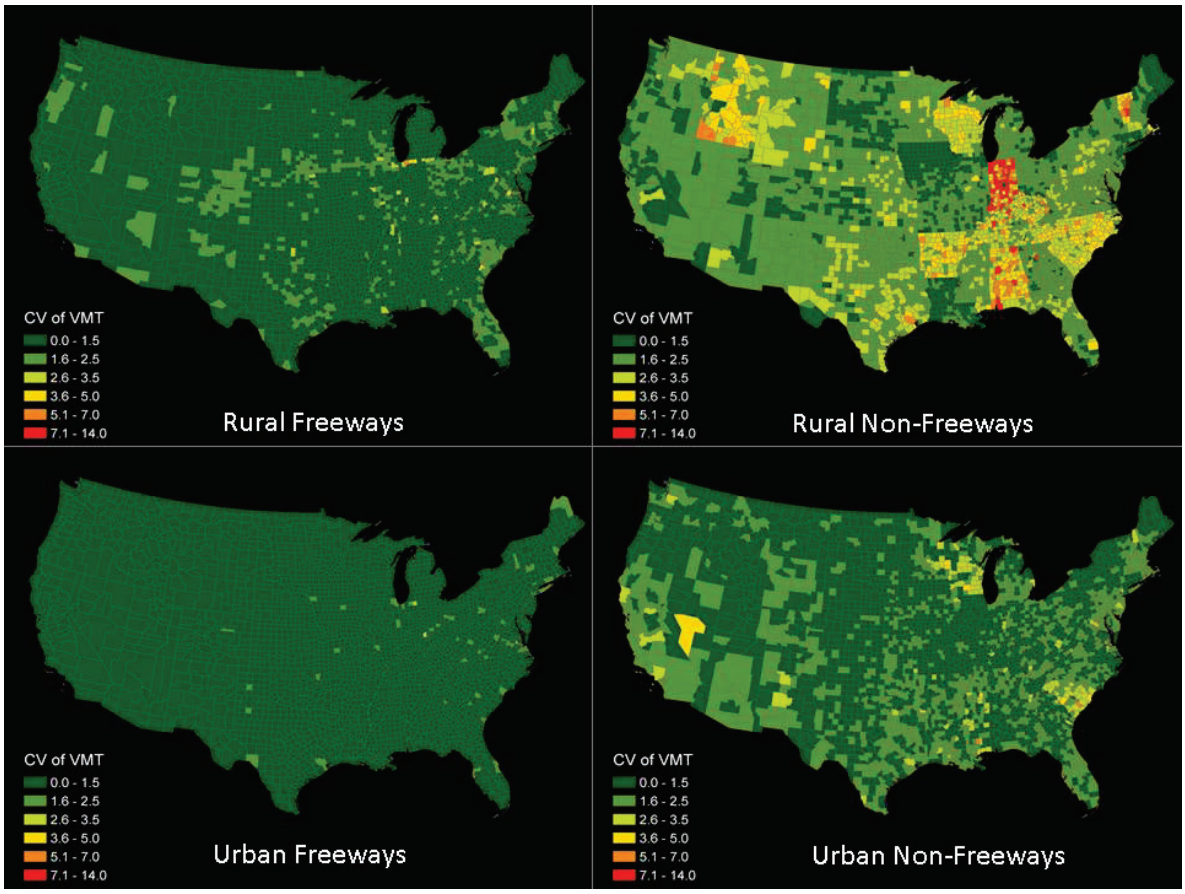

Figure S9. Within-county coefficient of variation (CV) of vehicles miles travelled by functional class, averaged over all years in the HPMS database.

At county and state scales the spatial imputation of AADT for roads that are not directly measured is another important source of uncertainty for VMT estimates. The imputation procedure consists of assigning traffic volumes to roads of similar functional class and urban/rural context using traffic counts measured on nearby roads. Large amounts of high resolution traffic data are needed to directly estimate the magnitude of this uncertainty. We calculated the within-state (between-county) coefficients of variation of VMT as a proxy measure of this spatial uncertainty. The CV of urban VMT ranged from 0.5 to 4.0 across all states and years, while rural VMT ranged more narrowly from 0.75 to 1.75 (Figure S10).The large variation in the state-level CVs of urban VMT reflects the broader range of urban area sizes at state scales, as small and large cities with different levels of vehicle activity fall into the same category of 'urban VMT' despite their inherent differences. The within-state CVs of emissions intensity (CO_2 / VMT) were small, ranging from 0.1 – 0.2 on average. Low variation in emissions relative to VMT is consistent with previous findings that uncertainty in vehicle fleet and fuel economy characteristics are a minor contributor to the overall uncertainty in emissions estimates from the on-road sector (16).

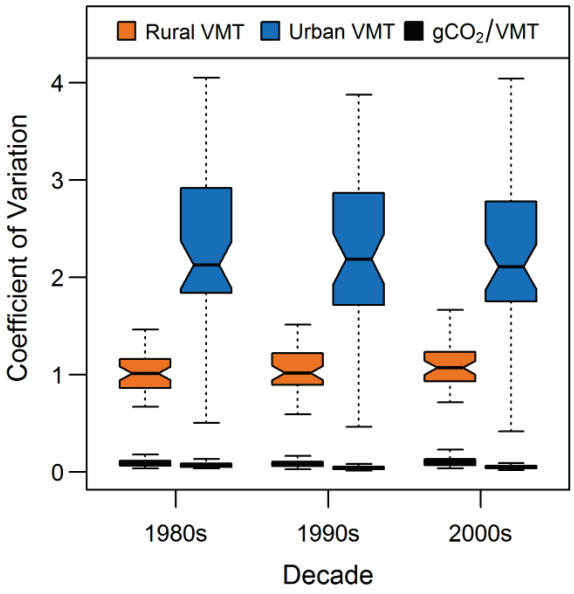

Figure S10. Coefficient of variation (CV) of intrastate VMT and emissions intensity (CO_2 per VMT) by decade. Each boxplot represents the distribution of CVs across all states. The CV for each state was calculated on the distribution of values for VMT and emissions intensity across all urban or rural roads in a state over each decade.

References for Supporting Information

1. Highway Performance Monitoring System Field Manual. Office of Highway Policy Information, Federal Highway Administration, Washington DC, 2010. URL: http://www.fhwa.dot.gov/ohim/hpmsmanl/hpms.htm
2. Highway Statistics Series, Table VM-2; 1980−2012; Federal Highway Administration: Washington, DC. http://www.fhwa.dot.gov/policyinformation/statistics Accessed July 1, 2013.
3. Highway Statistics Series, Table VM-4; 1980−2012; Federal Highway Administration: Washington, DC. http://www.fhwa.dot.gov/policyinformation/statistics Accessed July 1, 2013.
4. Highway Statistics Series, Table VM-1; 1980−2012; Federal Highway Administration: Washington, DC. http://www.fhwa.dot.gov/policyinformation/statistics Accessed July 1, 2013.

5. Highway Statistics Series, Table MF-21; 1980−2012; Federal Highway Administration: Washington, DC. http://www.fhwa.dot.gov/policyinformation/statistics Accessed July 1, 2013.
6. Vehicle Inventory and Use Survey; 1982-2002; U.S. Census Bureau: Washington, DC. https://www.census.gov/svsd/www/vius/products.html Accessed July 1, 2013.
7. Documentation for Emissions of Greenhouse Gases in the U.S. 2005, Table 6−1. DOE/EIA-0638 (2005); Energy Information Administration: Washington, DC, 2007.
8. Gurney KR, et al. (2009) High resolution fossil fuel combustion CO¬2 emission fluxes for the United States. *Environ Sci Technol*, 43, 5535-5541.
9. Emission Database for Global Atmospheric Research (EDGAR), release version 4.2; European Commission, Joint Research Centre (JRC)/Netherlands Environmental Assessment Agency (PBL), 2011; http://edgar.jrc.ec.europa.eu
10. Inventory of U.S. Greenhouse Gas Emissions and Sinks: 1990-2012. U.S. Environmental Protection Agency, Washington, DC, April, 2014. Report No. EPA 430-R-14-003.
11. Newman P, Kenworthy J (1989) Cities and Automobile Dependence: An International Sourcebook. Gower, Aldershot, UK.
12. U.S. Census Bureau; American Community Survey, 2010 American Community Survey 5-year Estimates, Table S0802; 2000 Census SF3 Sample Data, Table P030; Available at: factfinder2.census.gov. Accessed 08/01/14.
13. U.S. Census Bureau; Commuting and Journey to Work Data, 1990 Travel to Work Characteristics for the 50 Largest Cities in the United States by Population. Available at: https://www.census.gov/hhes/commuting/data/commuting.html Accessed on 08/01/14
14. Federal Highway Administration (2011). Summary of Travel Trends: 2009 National Household Travel Survey, Table 6. U.S. Department of Transportation, Washington, DC, June, 2011. Available at: http://nhts.ornl.gov/2009/pub/stt.pdf
15. Battelle Institute (2004) Traffic Data Quality Measurement−Final Report for the Office of Highway Policy Information; Federal Highway Administration, U.S. Department of Transportation: Washington, DC, September 15, 2004.
16. Mendoza D, et al. (2013) Implications of uncertainty on regional CO_2 mitigation policies for the US onroad sector based on a high-resolution emissions estimate. *Energy Policy*, 55, 386-395.